

Supporting Information

Efficient One-pot Valorization of Ethanol to 1-Butanol over Earth-abundant Ni-MgO Catalyst under Mild Conditions

Hao Wang^{a,b,&}, Gai Miao^{a,b,&}, Lingzhao Kong^{a,b,*}, Hu Luo^a, Yanfei Zhang^{a,b}, Xinpeng Zhao^{a,b}, Shenggang Li^{a,b,c,*},
Yuhan Sun^{a,b,c,*}

a. CAS Key Laboratory of Low-Carbon Conversion Science and Engineering, Shanghai Advanced Research Institute, Chinese Academy of Sciences, Shanghai 201210 (P.R. China). E-mail: konglz@sari.ac.cn, liscg@sari.ac.cn, sunyh@sari.ac.cn

b. University of Chinese Academy of Sciences, Beijing 100049 (P.R. China)

c. School of Physical Science and Technology, ShanghaiTech University, Shanghai 201203 (P.R. China)

&: These two authors contribute equally.

General Information

All chemicals were used as received from the commercial suppliers: Ethanol (GR, $\geq 99.8\%$), 1-butanol (GCS, $\geq 99.5\%$), Butyraldehyde (GCS, $\geq 99.5\%$), Ethyl acetate (GCS, $\geq 99.5\%$), 1,1-deithoxyethane (GCS, $\geq 99.5\%$), Ethyl butyrate (GCS, $\geq 99.5\%$), 1-hexanol (GCS, $\geq 99.5\%$), 2-ethyl-1-hexanol (GCS, $\geq 99.5\%$), 1-octanol (GCS, $\geq 99.5\%$), Acetone (AR, $\geq 99.8\%$), Na_2CO_3 (AR, $\geq 99.8\%$), $\text{Ni}(\text{NO}_3)_2 \cdot 6\text{H}_2\text{O}$ (AR, $\geq 98.0\%$), $\text{Mg}(\text{NO}_3)_2 \cdot 6\text{H}_2\text{O}$ (AR, $\geq 98.0\%$). All reactions were performed in a 50.0 mL Parr pressure reactor. Centrifugation of the reaction mixture was performed on Thermo LYNX6000 (3000 rpm, 5 min).

X-Ray powder diffraction (XRD) patterns of the catalysts were performed on Rigaku Ultima IV X-Ray diffractometer using $\text{Cu K}\alpha$ radiation in the 2θ range from 10° to 90° at a scan rate of $2^\circ \cdot \text{min}^{-1}$. Transmission electron microscopy (TEM) and energy dispersive X-ray spectrums (EDX) were performed on a JEM-2100F field emission electron microscope at an operating voltage of 200 kV equipped with a Gatan 832 CCD camera. Powdered samples were dispersed into ethanol solution under ultrasonic treatment for 40 min and the resulting suspension was put dropwise on a carbon film on copper grid. CO_2 -TPD and NH_3 -TPD were both conducted on Auto Chem. II2920 equipment (Micromeritics, USA). For CO_2 -TPD, 50 mg of sample was placed into a U-shaped quartz tube and heated from 50°C to 800°C at a ramping rate of $10^\circ\text{C}/\text{min}$ in a Helium atmosphere for 60 min and then cooled to 50°C in CO_2 gas for 60 min. Afterwards, heated from 50°C to 800°C at a ramping rate of $10^\circ\text{C}/\text{min}$ in a Helium atmosphere to desorb CO_2 . The data were recorded from 50°C to 800°C with a ramping rate of $10^\circ\text{C}/\text{min}$, and simultaneously monitored by a thermal conductivity detector (TCD). For NH_3 -TPD, 100 mg of sample was placed into a U-shaped quartz tube and heated from 50°C to 200°C at a ramping rate of $10^\circ\text{C}/\text{min}$ in an Argon atmosphere and then cooled to 50°C in NH_3 gas for 20 min, afterwards, heated from 50°C to 800°C at a ramping rate of $10^\circ\text{C}/\text{min}$ in an Argon atmosphere to desorb NH_3 . The data were recorded from 50°C to 800°C with a ramping rate of $10^\circ\text{C}/\text{min}$, and simultaneously monitored by a thermal conductivity detector (TCD). The contents of the metal Ni and Mg in the catalysts were measured using Inductively Coupled Plasma (ICP) on an Optimal Emission Spectrometer (Perkin Elmer Optima 8000). The Ni species were determined by X-ray Photoelectron Spectroscopy (XPS) on a Quantum 2000 Scanning ESCA Microprobe instrument with a monochromatic excitation source of Al $\text{K}\alpha$ radiation ($h\nu = 1486.6 \text{ eV}$) performed under 12 kV and 4 mA. H_2 temperature-programmed reduction (TPR) experiments were conducted on a Micromeritics Autochem II 2920 instrument equipped with a thermal conductivity detector (TCD) and an MKS Cirrus 2 mass spectrometer. Samples of 50 mg were first purged with Helium at a flow rate of 60 ml/min at 80°C for 1 h and then cooled down to 50°C . H_2 TPR was then conducted under Ar/H_2 by raising the temperature from 50 to 800°C at a rate of $10^\circ\text{C}/\text{min}$.

Analysis of Products

The data were recorded on the TRACE DSQ GC-MS (Agilent 7890GC and Agilent 5975C inert MSD). Analysis condition: column, 40°C for 3 min, increased from 40 to 120°C at $2^\circ\text{C}/\text{min}$ and held for 2 min, then increased from 120 to 250°C at $10^\circ\text{C}/\text{min}$, final temperature 250°C for 1 min. Column type: HP-5 (30 m, 0.25 mm inner diameter). After reaction, the solids were separated by filtration and the composition of the liquid phase was analyzed by GC-MS and GC-FID. Besides the main product 1-butanol, a variety of other compounds were detected, which were comprehensively analyzed. Compounds with a similarity match higher than 90% based on GC-MS identification accounted for a total area percentage $>95\%$ in all samples (Table S7). Quantification was carried out by GC-FID with the use of calibration curves and the calibrated compounds accounted for $>90\%$ of total products in all samples. Conversion and yield values were calculated based on the equations shown in the quantification part. During the reaction, the pressure produced an extra 5 bar at 250°C when cooling to room temperature which indicates the formation of volatile products during reaction as well. Main compounds in the gas phase included: methane, ethylene, ethane, H_2 , CO, and CO_2 .

Recycling Test

After a typical catalytic run (0.2g Ni-MgO, 15ml ethanol, 250°C , 5 h, 2.5 MPa helium), the catalyst was separated from the reaction solution by centrifugation and subsequent decantation. The solid was additionally washed with ethanol ($3 \times 10 \text{ ml}$), the with acetone ($1 \times 10 \text{ ml}$), and dried overnight at room temperature under vacuum prior to the next run.

Catalyst Preparation

The Ni-MgO catalyst precursors were prepared by a coprecipitation method. In a typical procedure, a solution containing $\text{Mg}(\text{NO}_3)_2 \cdot 6\text{H}_2\text{O}$ and $\text{Ni}(\text{NO}_3)_2 \cdot 6\text{H}_2\text{O}$ in deionized water (0.1 L) was slowly added to an aqueous solution (0.15 L) of Na_2CO_3 (0.025 mol, 1 g) at 70°C under vigorous stirring. The pH was carefully maintained between 9 and 10 by adjusting with frequent additions of an aqueous solution of Na_2CO_3 (1 M). The mixture was vigorously stirred for 4 h at 70°C . After cooling to room temperature, the suspension was filtered, and the solid was washed with deionized water. After the catalyst precursor was filtered, it was washed with deionized water until the washings were nitrate-free. The solid was dried at 80°C overnight, and the catalyst precursor was obtained as green powder. The collected powder was calcined under air atmosphere at increasing temperatures with a heating rate of $4^\circ\text{C}/\text{min}$ to 400°C and for 4 h at this temperature. The catalyst sample was reduced under H_2 atmosphere at increasing temperatures with a heating rate of $4^\circ\text{C}/\text{min}$ to 400°C at which it was kept for 4 h. Prior to exposure to air, the catalysts were passivated in a flow of 0.1% O_2/N_2 for 2 h at room temperature.

Quantification

The yield of products was calculated based on the number of carbon atoms in the product as follows: where n_i represents the number of carbons and C_i is the molar concentration of the compound i , C_{EtOH} indicates concentration of ethanol before the reaction.

$$Y_i(\%) = \frac{n_i C_i}{2C_{EtOH}} \times 100$$

Conversion was based on the number of carbon atoms in the compounds according to the equations below, where C_{EtOH} indicates concentration of ethanol before the reaction and C'_{EtOH} indicates concentration of ethanol after the reaction.

$$\text{Conversion}(\%) = \left(1 - \frac{C'_{EtOH}}{C_{EtOH}}\right) \times 100$$

It should be pointed out that we identified most of the products, as substantiated by the carbon balance average (ca. 90%). The carbon balance was calculated as follows:

$$C(\%) = \frac{2C'_{EtOH} + \sum_i n_i C_i}{2C_{EtOH}} \times 100$$

STY (time space yield) values illustrated mass of 1-butanol obtained in per unit time and unit catalyst mass, and the STY values can evaluate the activity of the catalyst. The STY values were calculated as follows and the unit was $\text{g}_{\text{but}}\text{kg}_{\text{cat}}^{-1}\text{h}^{-1}$: where t is reaction time, m is mass of 1-butanol and m' is mass of catalyst.

$$STY = \frac{m}{t * m'}$$

Conversion of Ethanol to 1-butanol

In a typical experiment, the catalyst (0.2 g unless otherwise stated) was placed in an intermittent high-pressure reactor (50 mL), and ethanol (15mL) were added. The reactor was sealed and placed in a heating sleeve at the desired temperature. After the indicated reaction time, the reactor was cooled down with an ice-water bath and subsequently carefully opened.

Table S1: Influence of temperature and catalyst loading on reaction performance using Ni-MgO catalyst

Temperature. (°C)	Cat. loading (g)	Carbon balance (%)	Conversion (%)	Yield/%							
				A	B	C	D	E	F	G	H
170	0.2	89.7	14.7	3.9	0.1	0.2	0.0	0.0	0.2	0.0	0.0
190	0.2	84.6	22.0	5.4	0.3	0.2	0.0	0.0	0.5	0.0	0.0
210	0.2	82.0	32.9	7.7	0.3	0.3	0.0	0.1	1.1	0.2	0.2
230	0.2	84.0	40.9	21.0	0.6	0.4	0.1	0.1	2.3	0.2	0.4
250	0.2	84.5	44.3	23.7	0.7	0.5	0.1	0.2	2.8	0.3	0.4
270	0.2	69.8	61.0	14.4	0.8	0.7	0.1	0.3	3.4	0.6	0.6
250	0.3	71.2	50.4	15.6	0.8	0.7	0.1	0.2	3.4	0.4	0.4
250	0.4	69.1	53.3	16.9	0.7	0.5	0.1	0.1	3.4	0.3	0.4
250	0.5	63.2	57.9	15.6	0.7	0.6	0.1	0.2	3.2	0.4	0.4

Reaction conditions : ethanol 15 ml, 5 h, 2.5 MPa helium. A: 1-butanol B: Butyraldehyde C: Ethyl acetate D: 1,1-deithoxyethane E: Ethyl butyrate F: 1-hexanol G: 2-ethyl-1-hexanol H: 1-octanol

Table S2: Examples of different catalysts for the conversion of ethanol to 1-butanol.

Catalyst	T(°C)	Device mode	Time (h)/ GHSV (ml/(h· g _{cat}))	Conversion (%)	1-butanol Yield (%)	STY (g _{but} kg _{cat} ⁻¹ h ⁻¹)	Ref.
MgO	450	Continuous	-	56.0	18.0	-	1
Mg ₃ AlO _x	350	Continuous	960 ml/(h· gcat)	35.0	14.0	-	2
Ca _{1.64} -P HAP	350	Continuous	880 ml/(h· gcat)	26.0	18.0	-	3
HAP	330	Continuous	820 ml/(h· gcat)	17.0	11.0	-	4
Sr _{1.7} -P HAP	300	Continuous	570 ml/(h· gcat)	11.0	9.0	-	5
PdMgAlO _x	200	Batch	5 h	3.8	2.9	369	6
CuMgAlO _x	200	Batch	5 h	4.1	1.6	203	7
Co Powder	200	Batch	72 h	4.0	2.9	8	8
Ni/Al ₂ O ₃	230	Batch	22.4 h	41.0	19.5	187	9
Ni/Al ₂ O ₃	250	Batch	72 h	27.0	22.0	79	10
Cu-CeO ₂	330	Continuous	-	67.0	30.0	-	11
Cu10Ni10-PMO	320	Batch	6 h	56.0	22.0	705	12
SrAp-100	400	Continuous	650 ml/(h· gcat)	13.0	8.2	-	13
Mg-Al	400	Continuous	-	37.1	12.4	-	14
HAP	340	Continuous	720 ml/(h· gcat)	5.0	3.2	-	15
Cu/Mg/Al-HTC	320	Batch	6 h	64.0	29.0	767	16
Ru+NaOEt	150	Batch	4 h	46.0	32.0	1209	17
Cu+MgO	230	Batch	12 h	32.4	16.9	147	18
CaC ₂	275	Batch	6 h	46.0	19.5	174	19
Calcium ethoxide	300	Batch	8 h	25.0	10.8	36	20
Cu10MMO	350	Batch	5 h	79.6	25.4	-	21
RuNi@MOF	170	Batch	14.5 h	6.2	4.8	-	22
Pd@UiO-66	250	Continuous	-	49.8	24.2	-	23
Ni-MgO	250	Batch	5 h	44.3	23.7	1880	This work

Table S3: Catalyst recycling experiments.

Cycles	Conversion/%	Yield/%							
		A	B	C	D	E	F	G	H
1	44.3	23.7	0.7	0.5	0.1	0.2	2.8	0.3	0.4
2	39.4	19.5	0.5	0.4	0.1	0.1	2.2	0.2	0.4
3	39.1	18.3	0.5	0.4	0.1	0.1	2.2	0.2	0.4
4	39.9	19.0	0.5	0.4	0.1	0.1	2.2	0.2	0.4
5	38.8	17.5	0.5	0.4	0.1	0.1	2.2	0.2	0.3
6	39.5	17.6	0.5	0.4	0.1	0.1	2.2	0.2	0.3
Regeneration	42.1	21.8	0.6	0.4	0.1	0.1	2.3	0.2	0.4

Reaction conditions : Ni-MgO 0.2g, ethanol 15 ml, 250 °C, 5 h, 2.5 MPa helium. A: 1-butanol B: Butyraldehyde C: Ethyl acetate D: 1,1-deithoxyethane E: Ethyl butyrate F: 1-hexanol G: 2-ethyl-1-hexanol H:1-octanol

Table S4: Leaching tests during catalyst recycling for Ni-MgO catalyst.

Cycles	Ni(mg/L)	Mg(mg/L)
Before reaction	14.2	5.9
1	11.6	4.7
6	11.3	4.6

Table S5: Results of the MgO, Ni-MgO, Ni10-MgO, Ni0.1-MgO in the Guerbet reaction of ethanol to 1-butanol

Catalysts	Carbon balance (%)	STY ($\frac{g_{but}}{kg_{cat} \cdot h}$)	Conversion/%	Yield/%							
				A	B	C	D	E	F	G	H
MgO	89.9	767	35.6	7.2	1.0	0.4	0.0	0.1	1.7	0.1	0.3
Ni-MgO	84.5	1880	44.3	23.7	0.7	0.5	0.1	0.2	2.8	0.3	0.4
Ni10-MgO	73.6	428	47.4	5.4	1.1	0.3	0.0	0.1	1.3	0.1	0.3
Ni0.1-MgO	88.6	1063	42.7	13.4	0.6	0.5	0.1	0.1	2.0	0.1	0.2

Reaction conditions : catalysts 0.2 g , ethanol 15 ml, 250 °C, 5 h, 2.5 MPa helium. A: 1-butanol B: Butyraldehyde C: Ethyl acetate D: 1,1-deithoxyethane E: Ethyl butyrate F: 1-hexanol G: 2-ethyl-1-hexanol H: 1-octanol

Table S6: Acid–base properties of the MgO and different Ni-MgO catalysts determined by CO₂-TPD and NH₃-TPD

Catalysts	STY ($\text{g}_{\text{but}}\text{kg}_{\text{cat}}^{-1}\text{h}^{-1}$)	Number of basic sites($\mu\text{mol/g}$)	Number of acid sites($\mu\text{mol/g}$)
MgO	767	346.3	382.9
Ni0.1-MgO	1063	390.6	351.0
Ni-MgO	1880	487.1	700.7
Ni10-MgO	428	173.3	432.7
Ni-MgO(uesd)	1547	415.6	718.5

Table S7: GC-MS analysis of the products.

Retention time (min.)	Area Percentage %	Compound name	Similarity
1.453	0.13	Propane	90
1.519	0.99	Acetaldehyde	91
*1.632	47.10	Ethanol	93
*2.082	1.29	Butanal	96
*2.213	1.59	Ethyl Acetate	91
*2.818	28.16	1-butanol	91
3.010	0.35	2-pentanone	87
3.112	0.49	Heptane	87
3.399	0.23	Propanoic acid, ethyl ester	87
*3.758	0.77	Ethane, 1,1-diethoxy-	83
4.435	0.23	Butanal, 2-ethyl-	91
5.118	0.32	3-hexanone	97
5.567	0.17	Hexanal	97
*5.645	0.54	Butanoic acid, ethyl ester	94
6.148	0.30	Acetic acid, butyl ester	83
7.196	0.05	1-butanol, 2-ethyl-	90
*8.603	7.45	1-hexanol	90
9.783	0.16	Nonane	94
*17.862	2.05	1-hexanol, 2-ethyl-	90
*20.766	2.60	1-octanol	90
31.432	0.19	2-hexyl-1-octanol	90
34.558	0.17	Dichloroacetic acid, dodecyl ester	81
50.452	0.30	N,N-diethyl-p-nitroaniline	80
53.260	0.41	Benzenesulfonamide, n-butyl-	97

Reaction conditions: Ni-MgO 0.2 g, ethanol 15 ml, 250 °C, 5 h, 2.5 MPa helium

*: compounds further confirmed by spiking with authentic standards. Quantification was performed based on additional GC-FID analysis using internal standard and calibration curves for compounds labeled with *

Only compounds with a similarity match higher than 80% based on GC-MS identification are listed. These accounted for a total area percentage >95%.

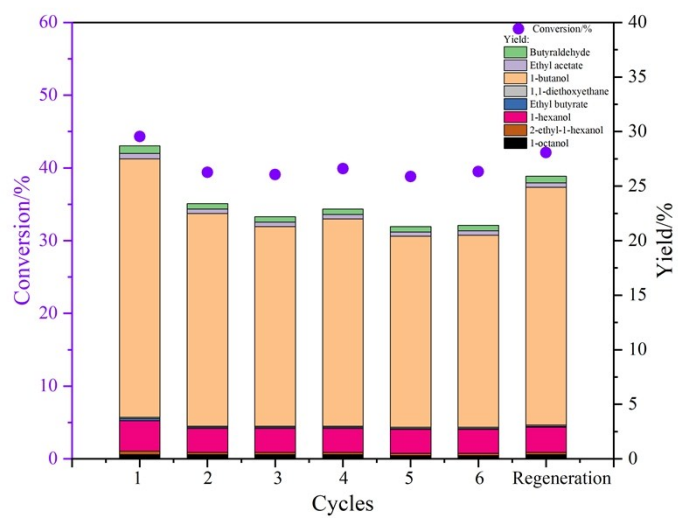
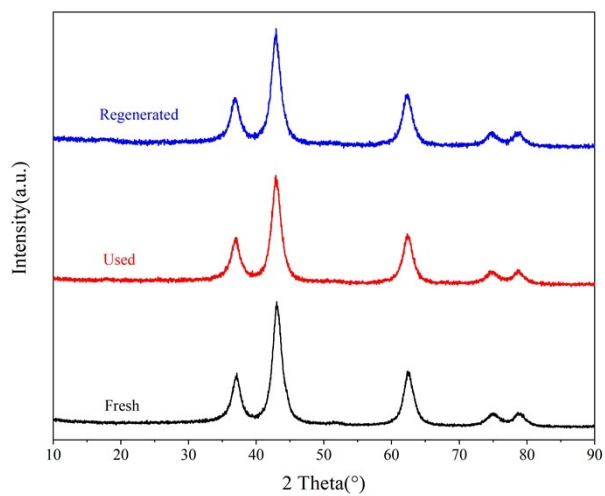
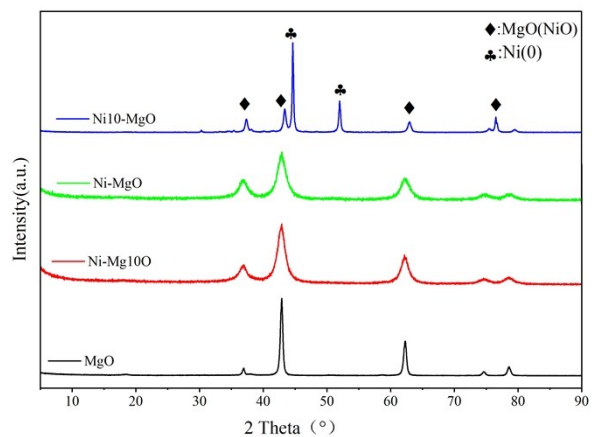


Fig. S1: Recycling test. Reactions: Ni-MgO (200 mg), ethanol (15 ml), 250 °C, 5 h, 2.5 MPa helium.



(a)



(b)

Fig. S2: (a): XRD patterns of the fresh, used and regenerated Ni-MgO catalyst by calcination at 400 °C for 4 h; (b): XRD patterns of the MgO, Ni0.1-MgO, Ni-MgO and Ni10-MgO catalysts.

As was shown in the XRD pattern of fresh Ni-MgO catalyst (Fig. S2 b), the Ni(0) was not observed compared with Ni10-MgO, which can be explained by the appearance of the NiO-MgO solid solution to be reduced and small crystallite sizes of Ni(0) particles generated from the NiO phase. And the XRD pattern of fresh Ni10-MgO catalyst showed the apparent Ni(0) peak at 2 Theta=45.2, 52.7.

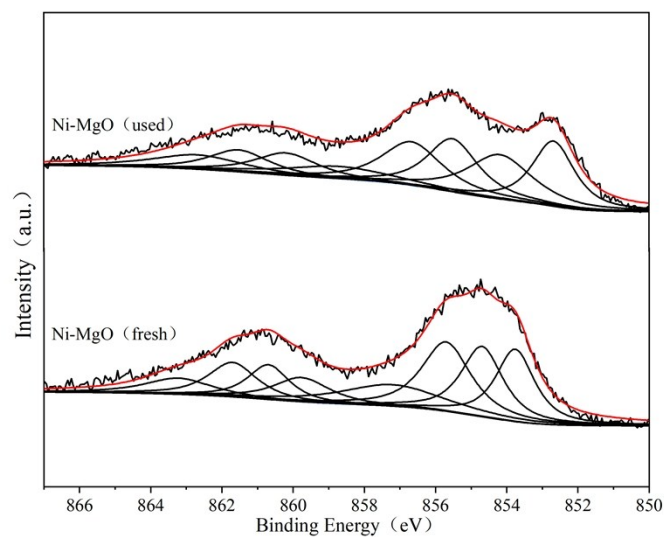


Fig. S3: The Ni $2p_{3/2}$ spectrum for fresh and used Ni-MgO catalysts.

Fig. S3 shows the Ni $2p_{3/2}$ spectra of fresh and used Ni-MgO catalysts, which contains the main peaks of multiplet set with nickel species at 853.7 eV, ~854.2 eV, ~855.6 eV, ~857.0eV, and their satellite peaks by 6.0eV above the main line. The main line peaks was assigned Ni(0)²⁴, NiO²⁵, Ni(OH)₂²⁶, Ni(OH)₂/MgNi_x²⁷. Here, the nickel species was classified by two categories: Ni(0) and Ni(2+). Ni(2+) includes NiO and Ni(OH)₂ species. By integrating the main peak area, the ratio of Ni(0) for fresh Ni-MgO is 24.6% and that for used Ni-MgO is 24.9%. The ratio of Ni(0)/Ni(2+) for fresh and used Ni-MgO catalysts are similar.

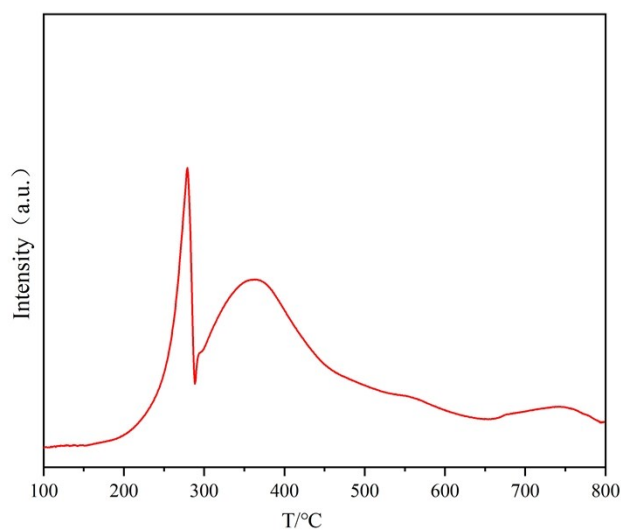


Fig. S4: The H₂-TPR curves of the calcined Ni-MgO catalyst.

The H₂ TPR profiles of calcined Ni-MgO were shown in the Fig. S4. The peak at 260 °C and 370 °C in the TPR profile of Ni/MgO could be attributed to the reduction of bulk NiO particles on the MgO surface. The broad consumption of hydrogen over 650 °C might be assigned to the reduction of Ni²⁺cations inserted into the lattice of MgO due to the formation of a solid solution during calcination. Considering the H₂-TPR profiles, the reduction temperature used for the preparation of the Ni-MgO catalysts was chosen as 400 °C, in order to reduce NiO particles, although this temperature is not enough for reducing Ni²⁺in the solid solution, and minimize metal sintering²⁸⁻³¹.

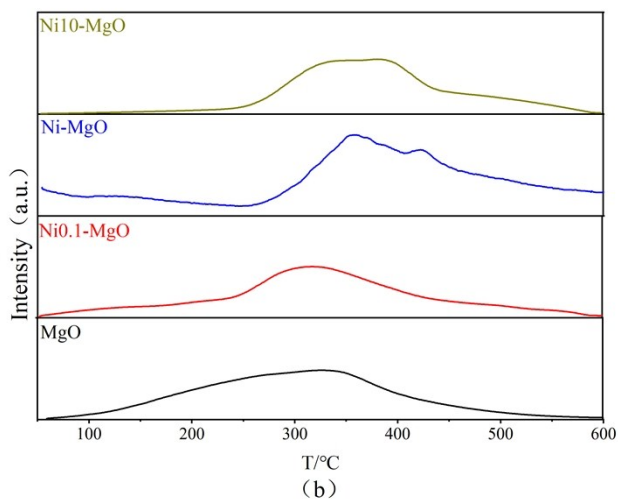
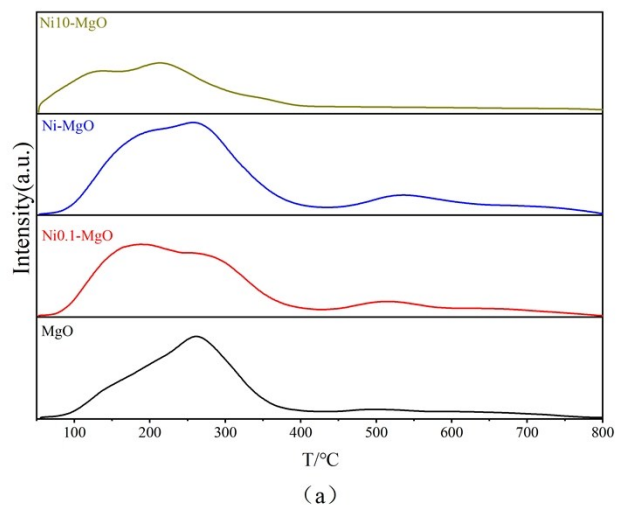


Fig. S5: CO₂-TPD (a) and NH₃-TPD (b) profiles of the investigated catalysts.

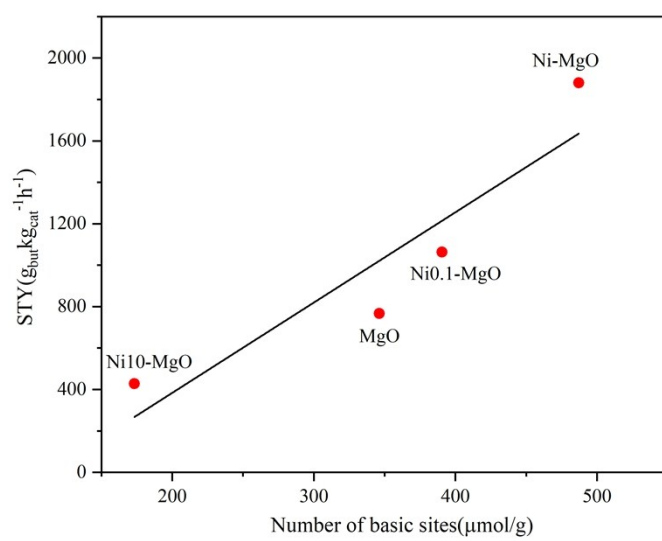


Fig. S6: The relation of STY values and numbers of basic sites in MgO, Ni0.1-MgO, Ni-MgO and Ni10-MgO catalysts.

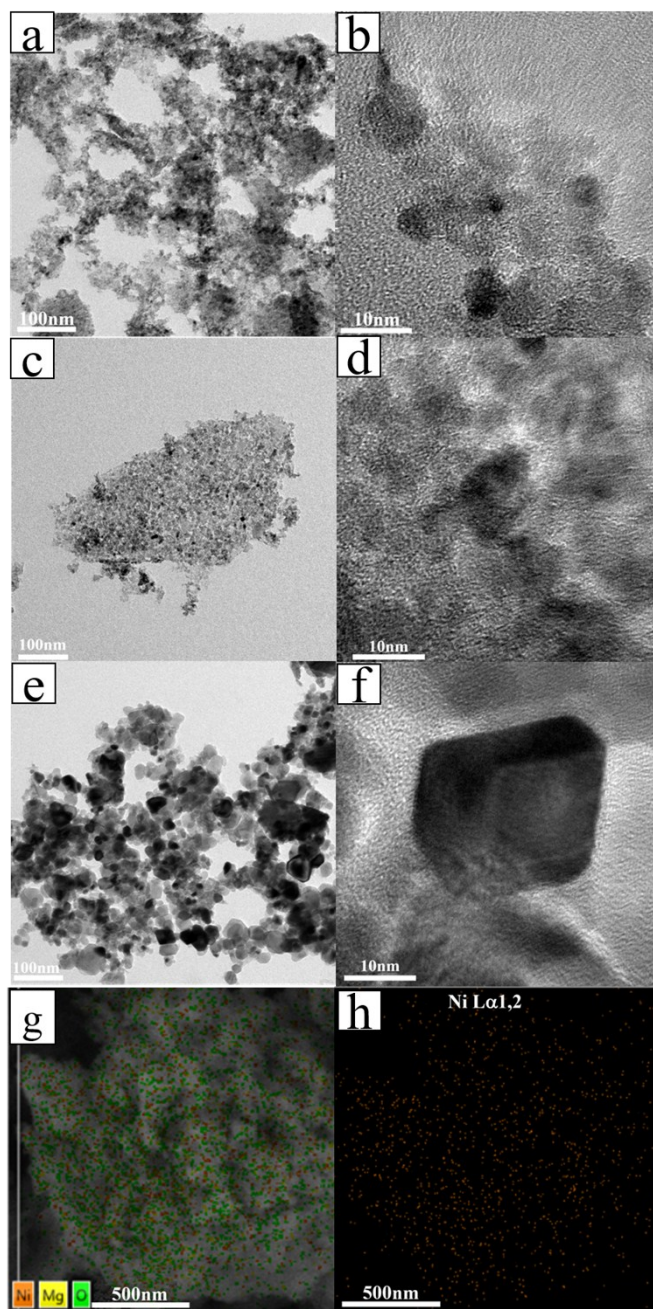


Fig. S7: TEM images of the fresh Ni-MgO (a, b), Ni_{0.1}-MgO (c, d) and Ni₁₀-MgO(e,f) catalysts, EDS(g) and Ni element mapping (h) of the fresh Ni-MgO.

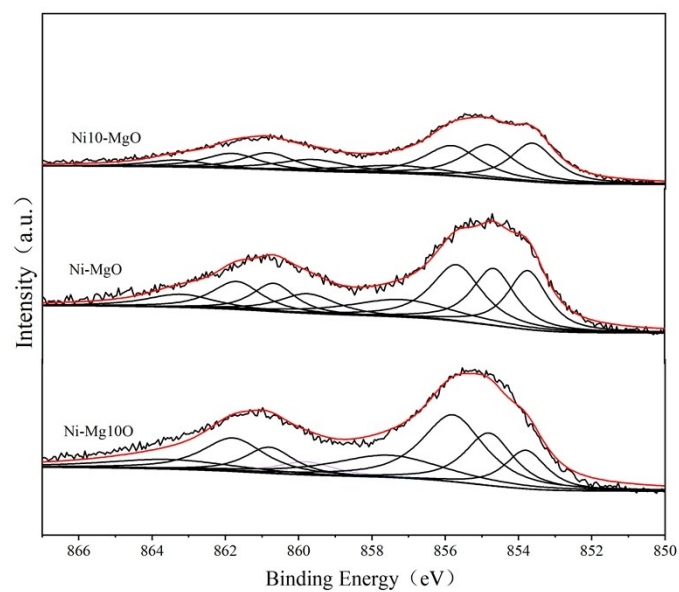


Fig. S8: The Ni $2p_{3/2}$ spectrum of Ni10-MgO, Ni-MgO and Ni0.1-MgO catalysts.

Using the same analysis method in Fig. S3, the ratio of Ni(0) for Ni10-MgO is 28.4% and that for used Ni-MgO is 24.9%. In Ni0.1-MgO catalyst, due to the low loading of Ni on the MgO support, the ratio of Ni(0) drops to 14.7%. Except for the Ni(0) species, the others are Ni(2+) species, including NiO and Ni(OH)₂.

Reference:

- 1 A. S. Ndou, N. Plint and N. J. Coville, *Appl. Catal. A-Gen.*, 2003, **251**, 337-345.
- 2 D. L. Carvalho, R. R. de Avillez, M. T. Rodrigues, L. E. P. Borges and L. G. Appel, *Appl. Catal. A-Gen.*, 2012, **415**, 96-100.
- 3 T. Tsuchida, S. Sakuma, T. Takeguchi and W. Ueda, *Ind. Eng. Chem. Res.*, 2006, **45**, 8634-8642.
- 4 C. R. Ho, S. Shylesh and A. T. Bell, *ACS Catal.*, 2016, **6**, 939-948.
- 5 S. Ogo, A. Onda, Y. Iwasa, K. Hara, A. Fukuoka and K. Yanagisawa, *J. Catal.*, 2012, **296**, 24-30.
- 6 I. C. Marcu, N. Tanchoux, F. Fajula and D. Tichit, *Catal. Lett.*, 2013, **143**, 23-30.
- 7 I. C. Marcu, D. Tichit, F. Fajula and N. Tanchoux, *Catal. Today*, 2009, **147**, 231-238.
- 8 X. L. Zhang, Z. W. Liu, X. L. Xu, H. J. Yue, G. Tian and S. H. Feng, *ACS Sustain. Chem. Eng.*, 2013, **1**, 1493-1497.
- 9 T. L. Jordison, C. T. Lira and D. J. Miller, *Ind. Eng. Chem. Res.*, 2015, **54**, 10991-11000.
- 10 T. Riittonen, E. Toukoniitty, D. K. Madnani, A. R. Leino, K. Kordas, M. Szabo, A. Sapi, K. Arve, J. Warna and J. P. Mikkola, *Catalysts*, 2012, **2**, 68-84.
- 11 J. H. Earley, R. A. Bourne, M. J. Watson and M. Poliakoff, *Green Chem.*, 2015, **17**, 3018-3025.
- 12 Z. H. Sun, A. C. Vasconcelos, G. Bottari, M. C. A. Stuart, G. Bonura, C. Cannilla, F. Frusteri and K. Barta, *ACS Sustain. Chem. Eng.*, 2017, **5**, 1738-1746.
- 13 L. Silvester, J. F. Lamonier, C. Lamonier, M. L. Capron, R. N. Vannier, A. S. Mamede and F. Dumeignil, *ChemCatChem*, 2017, **9**, 2250-2261.
- 14 J. Quesada, L. Faba, E. Diaz and S. Ordonez, *Appl. Catal. A-Gen.*, 2017, **542**, 271-281.
- 15 Z. D. Young and R. J. Davis, *Catal. Sci. Technol.*, 2018, **8**, 1722-1729.
- 16 J. A. Barrett, Z. R. Jones, C. Stickelmaier, N. Schopp and P. C. Ford, *ACS Sustain. Chem. Eng.*, 2018, **6**, 15119-15126.
- 17 R. Mazzoni, C. Cesari, V. Zanotti, C. Lucarelli, T. Tabanelli, F. Puzzo, F. Passarini, E. Neri, G. Marani, R. Prati, F. Viganò, A. Conversano and F. Cavani, *ACS Sustain. Chem. Eng.*, 2019, **7**, 224-237.
- 18 P. Benito, A. Vaccari, C. Antonetti, D. Licursi, N. Schiaroli, E. Rodriguez-Castellon and A. M. R. Galletti, *J. Clean Prod.*, 2019, **209**, 1614-1623.
- 19 D. Wang, Z. Y. Liu and Q. Liu, *RSC Adv.*, 2019, **9**, 18941-18948.
- 20 D. Wang, Z. Y. Liu and Q. Y. Liu, *J. Phys. Chem. C*, 2019, **123**, 22932-22940.
- 21 M. R. Siqueira, O. M. Perrone, G. Metzker, D. C. D. Lisboa, J. C. Thomeo and M. Boscolo, *Mol. Catal.*, 2019, **476**, 8.
- 22 C. N. Neumann, S. J. Rozeveld, M. Yu, A. J. Rieth and M. Dinca, *J. Am. Chem. Soc.*, 2019, **141**, 17477-17481.
- 23 D. H. Jiang, G. Q. Fang, Y. Q. Tong, X. Y. Wu, Y. F. Wang, D. S. Hong, W. H. Leng, Z. Liang, P. X. Tu, L. Liu, K. Y. Xu, J. Ni and X. N. Li, *ACS Catal.*, 2018, **8**, 11973-11978.
- 24 S.O. Grim, L.J. Matienzo and W.E. Swartz, *J. Am. Chem. Soc.* 1972,**94**, 5116.
- 25 V.I. Nefedov, M.N. Firsov and I.S. Shaplygin, *J. Electron Spectrosc. Relat. Phenom.* 1982, **26**, 65.
- 26 A.M. Venezia, R. Bertonecello and G. Deganello, *Surf. Interface Anal.* 1995,**23**, 239.
- 27 P. Selvam, B. Viswanathan and V. Srinivasan, *J. Electron Spectrosc. Relat. Phenom.* 1989,**49**, 203.
- 28 C. P. Jimenez-Gomez, J. A. Cecilia, C. Garcia-Sancho, R. Moreno-Tost and P. Maireles-Torres, *ACS Sustain. Chem. Eng.*, 2019, **7**, 7676-7685.
- 29 R. K. Singha, A. Shukla, A. Sandupatla, G. Deo, R. Bal, *J. Mater. Chem. A*, 2017, **5**, 15688-15699.
- 30 F. Frusteri, S. Freni, V. Chiodo, S. Donato, G. Bonura, S. Cavallaro, *Int. J. Hydrogen Energ.*, 2006, **31**, 2193-2199.
- 31 G. T. Wurzler, R. C. Rabelo-Neto, L. V. Mattos, M. A. Fraga, F. B. Noronha, *Appl. Catal., A*, 2016, **518**, 115-128.